



Case of Study on Particle Shape and Friction Angle on Tailings

Juan M. Rodriguez and Tommy Edeskär
Luleå University of Technology, Sweden
SE-971 87 LULEÅ, Sweden

Juan.rodriquez@ltu.se, Tommy.edeskar@ltu.se

ISSN 2231-8844

Article Info

Received: 10/6/2013
Accepted: 28/8/2013
Published online: 1/9/2013

Abstract

Tailings are crushed and milled materials result of the mining production. Tailings need to be stored in facilities, usually tailings dams, for a long time period for mainly safety and environmental protection. In order to design tailings dams in a long term perspective not only current material properties is needed but also future changes of these properties due to e.g. weathering. On a particle level the weathering will result in shape changes and decomposition. By studying the changes in shape a prognosis of changes in properties of a tailings deposit may be established. Tailings are site specific material and are not well investigated compared to natural geological materials such as soil. Tailings materials size ranges generally from sand to silt and the particle shape by genesis or production processes. Based on laboratory tests tailings from the Aitik mine has been investigated through triaxial tests and particle shape quantification by two dimensions image analysis. The shape descriptors Aspect Ratio, Circularity, Roundness and Solidity are used in this study. These shape descriptors are evaluated based on how well these describes talings materials. The evaluated shape descriptors are used in previous published empirical relations between shape and friction angle. As reference are friction angles evaluated by triaxial tests on the material used. The results show that the particle shape is affected by the size of the aggregates. Aggregates in small fractions are more elongated and less rounded, i. e. more angular, compared to larger. Furthermore, the Aspect Ratio and Circularity seems to be the most situable quantities to describe the tailings behaviour in relation with the empirical model. The accuracy in predicting the friction angle of the tailings by previously published relations based on uniformly graded sand material are low. But the systematic underestimation of the friction angle indicates that it would be possible to establish such empirical relations based on tailings material.

Keywords: Particle shape, Quantities, Image analysis, Friction angle.

1 Introduction

Tailings are crushed and milled by products from ore refining and generally considered to be angular aggregates in the size range from silt to fine sand (FHA, 1997). From an engineering perspective in general the strength and deformations properties of the tailings are regarded as a natural soil material in the same size range and size distribution.

Garga et. al. (1984) classifies the shape of tailings to be in the range from angular to sub angular. The high angularity contributes to high initial friction angles and, as a consequence of the deposition methods to high void ratio and loose fills (Holubec and D'Appolonia, 1973; Rousé et. al., 2008, among others). It is also likely that physical (e.g. stresses) and chemical (e.g. oxidation) weathering in a long time perspective will result in less angular aggregates. Yoginder et. al. (1985) show that angular aggregates are more sensitive to shape changes due to edge breakage and subsequently generation of fines under increasing confining stress compared to natural geological material. Physical properties e.g. the friction angle are shape dependent and a reduction in angularity will reduce the friction angle (Cho et. al., 2006). Empirical relations have been suggested by authors as Cho et. al. (2006) and Rousé et. al. (2008) in studies where the friction angle (from triaxial tests) and particle *Roundness* according to Wadell (1932)-definition are correlated. Uniform graded soil samples, basically sand, were used to determine these empirical relations. The tailings investigated in this study contain a wider range of particle sizes and especially more fine graded fractions such as silt and clay compared to these studies. The selection of comparative empirical relations for predicting the friction angle is based on the laboratory test procedure (triaxial tests) and the range of friction angle covered by these suggested relations.

Depending on the mineral composition and the deposition conditions chemical weathering may be an important factor to account for in a long time perspective. e.g. sulphide rich tailings are highly susceptible to oxidize due to the large surface exposure of the grains. Furthermore the presence of oxygen and water (no saturated) provide an adequate environment for sulphuric acid production (Al-Rawahy, 2001) that could foment the increase of oxidation and also promotes the particles shape change. If tailings dams are considered to be designed as “walk-away”-solution or to be safe in a thousand year perspective it is important to account for both the change in properties and the consequential global effect on the tailings dam.

There are more than 40 quantities (shape descriptors) compiled in the report by Rodriguez et. al. (2012) able to determine the particle shape, but there has been only minor efforts to evaluate the suitability among these descriptors in relation with the effect on the soil properties. Authors such as e.g. Cheshomi et. al. (2009) and Cho et. al. (2006) had used the comparison chart develop by Krumbein and Sloss (1963). According to Folk (1955) there is an appreciation error involve in chart comparison as methodology. The lack of possibility to objectively describe the shape hinders the development of incorporating the effect of particle shape in geotechnical analysis. Computer algorithms had been developed for at least half of the quantities and the use of image analysis reduces dramatically the processing time and provides reproducibility.

In this work *Aspect Ratio (AR)*, *Roundness (R)*, *Circularity (C)* and *Solidity (S)* were chosen quantities to analyze trough image analysis software.

2 Scope of study

The scope of the study is to describe tailings by shape and relate the shape as indicative measure for physical properties. The aims of the study are to classify tailings by shape using 2D image analysis technique in a case study on tailings from Aitik. The classified tailings by different shape factors are correlated to the friction angle by applying previously published empirical relations based on soil material compared with triaxial test results on the tailings material in order to investigate if this methodology could be applicable as indicative measure of physical properties on tailings.

3 Methodology

In this study has tailings from Boliden's mine Aitik outside Gällivare in northern Sweden been analyzed. The target minerals are mainly copper and gold and the ore is of sulphide type. The analysis includes basic geotechnical characterization and particle analysis. The geotechnical characterization includes sieving, compact density test and active triaxial tests. The analysis of the individual particles has been done by image analysis for shape description and x-ray analysis for classification of oxidation potential. The results from the particle shape description and laboratory results are compared with previous published empirical results on the effect of particle shape on strength properties.

Undisturbed samples have been collected by coring. Four samples were analyzed from Aitik tailing dam. Two of the samples are located in the surrounding area of the corner of the tailings dam bodies where GH-EF meets as shown in figure 1.

- I, Position: 61+900@150m. Samples "a" and "b".
- II, Position: 62+643@150m. Samples "c" and "d"

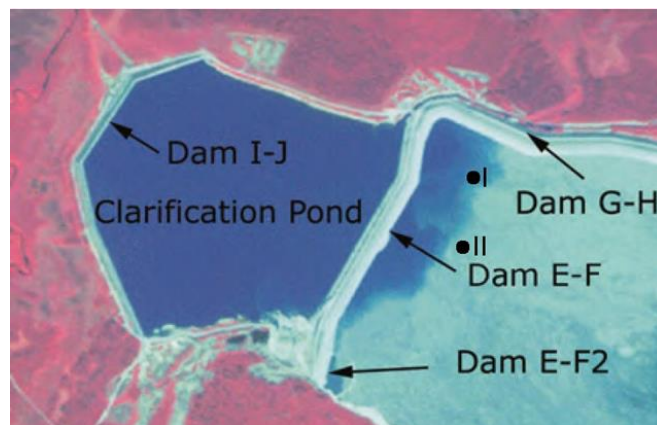


Figure 1: Aerial view of part of the Aitik Tailings dam to the right in the picture sampling locations (I) and (II).(Photo courtesy of Boliden Mineral AB.)

3.1 Geotechnical characterization and triaxial tests

The sampled material was characterized by sieving, ocular inspection, determination of water quotient, compact density and bulk density.

Active triaxial test were performed on three samples in a confining stress-ranges of 90-150 kPa in undrained conditions (see table 1). One sample was executed in drained conditions. The samples used were retrieved by undisturbed coring. After basic characterization of the cores the triaxial tests were performed. The used triaxial equipment used was GDS Instruments based on Bishop and Wesleys (1975) principle of triaxial apparatus. The samples had, been step by step, isotropic confined. During this consolidation a backpressure of 100 kPa has been applied. In the case a maximal deviatoric stress (peak) was registered during shearing the friction angle was evaluated at both the maximal deviatoric stress and at the residual stresses. For those samples where a maximal deviatoric stress was not registered the friction angle was evaluated at 15 % compression was used.

Table 1. Triaxial tests used in this study.

Location	Id	Sampling depth [m]	Triaxial test	Confining pressure [kPa]
I	a	13.3	Drained	140
I	b	13.3	Undrained	150
II	c	8.3	Drained	90
II	d	16.8	Drained	170

3.2 Visual inspection and X-ray

Visual inspection was performed using the undisturbed samples under a traditional magnification lens. For the X-ray test the PANalytical Empyrean X-ray Diffractometer equipped with PIXcel3D detector and X-ray tube Empyrean Cu LFF HR was used.

3.3 Image analysis

One fraction of each undisturbed cored samples was used to obtain the grains subject to image generation. In order to obtain clear images it was needed to sieve each fraction sample by wet sieve in five standard sieves mesh (1, 0.5, 0.25, 0.125 and 0.063mm). The particle size separation provides better focus in the microscope. The used microscope was *Motic B1*, with two lenses used with magnification rates of 4x and 10x (for particle size of 0.063mm). The camera mounted on top of the microscope (*Infinity 2*) and has a 2 megapixel resolution. It is equipped with lightening sources from below (straight light from source to lens) and external lightening able to move and locate in any position. The external lightening source was chosen (also from the bottom of the sample) due the possibility of change the light directional angle. The ability to have a non-unidirectional light source provide good contrast in the particle's outline specially in mica minerals (light passes through easily) that usually are not well defined and there is not enough contrast when unidirectional light is applied. A total of 160 to 300 of particles (approximated) by sample were measured (see Appendix).

Table 2. Shape describing quantities and their mathematical definitions

Eq. #	Quantity	Definition	Reference	Eq. #	Quantity	Definition	Reference
1	Circularity (C)	$\frac{4\pi A}{P^2}$	Cox (1927)	2	Roundness (R)	$\frac{4A}{\pi Major^2}$	Ferreira And Rasband (2012)
3	Solidity (S)	$\frac{A}{A_c}$	Mora And Kwan (2000)	4	Aspect Ratio (Ar)	$\frac{Major}{Minor}$	Ferreira And Rasband (2012)

A, Area
 A_c, Area Convex
 P, Perimeter
 Major, Major Axis Based On Fitting Ellipse
 Minor, Minor Axis Based On Fitting Ellipse

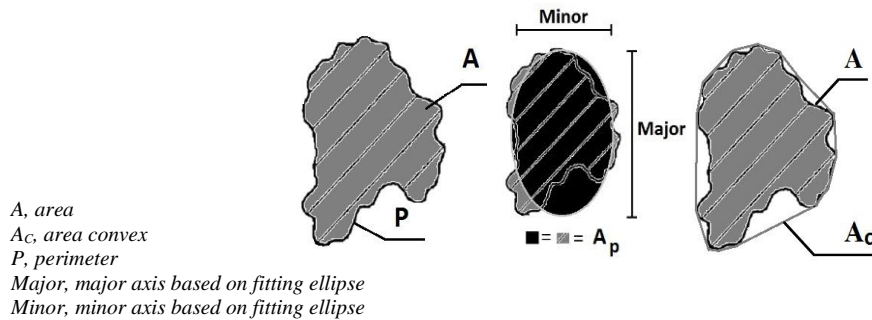


Figure 2: Definition of the quantities applied in this study. From left: Circularity (C), Roundness (R), and Solidity (S).

Images were analyzed with software ImageJ and four descriptors were determined: *Aspect Ratio (AR)*, *Roundness (R)*, *Circularity (C)* and *Solidity (S)*. The definitions of these quantities are presented in table 2 and figure 2.

3.4 Correlation of shape descriptors by physical properties

A set of four databases were compiled, each database correspond to one triaxial test sample. Each database contains values for the four quantities (see Appendix) and the five sieving ranges (1, 0.5, 0.25, 0.125 and 0.063mm). Similar statistical analysis was performed among the four databases as follow: the minimum and maximum values for each quantity along the five sieving sizes per sample were obtained. Average values were obtained from each size range per sample and quantity. Median values for each sieve size were also obtained per sample. The quantity values were applied in the empirical relations in table 3, to investigate if this methodology could be useful for prediction of indicative physical properties.

Table 3. Empirical relations suggested in literature relating the friction angle (ϕ') and the shape quantity (Q).

EQ. #	DEFINITION	REFERENCE
5	$\phi' = 42 - 17Q$	Cho et. al. (2006)
6	$\phi' = 41.7 - 14.4Q$	Rousé (2008)
<i>Q, quantity value (0 to 1)</i>		

4 Results

4.1 Geotechnical characterization and triaxial tests

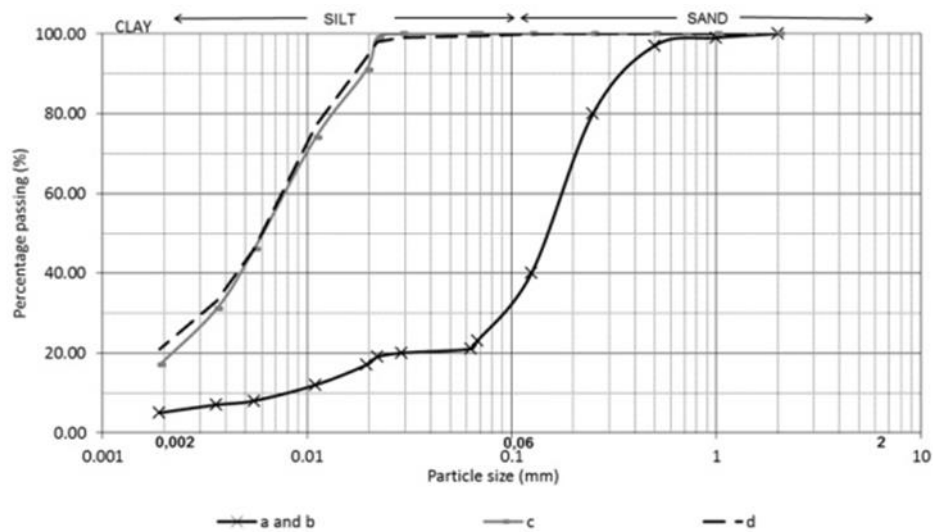


Figure 3. Sieving curves for the Aitik tailing samples (SWECO Geolab, 2007)

The samples are classified as silt, with the exception of *a* and *b* that is a sand-silt material (see sieving curve fig. 3). The sieving curves *a* and *b* are based on other samples than used in the triaxial tests but from corresponding depth, 12.2m. The amount of clay, or fines, ranges up to 20 % of the samples.

Ocular inspection on the samples shows the presence of mica, except sample *c*. In this sample some oxidation is recognized consisting of reddish colored zones. The red color is presumed to be the result of the iron oxidation coming from pyrite and chalcopyrite that is commonly present in the tailings. The X-ray tests also show the presence of mica (biotite and muscovite).

The results from the basic geotechnical characterization and the triaxial tests are compiled in table 4. As seen in the table the result of an evaluation of the friction angle by Mohr-Coloumb failure criterion will generate high difference depending on a cohesion intercept is used or if the cohesion intercept is omitted ($c=0$ kPa). By inspection of the samples the material could be considered to have low or moderate cohesion depending on the clay content. Thus is the approximation of the failure envelope to be straight, as in the Mohr-Coloumb failure criterion, not valid for high stress intervals, or at least for the lower ranges of effective stress. The initially loose specimens has equally high, or higher friction angle compared to the firm. Dilatant behavior during shearing was observed for all the initially firm specimens including the undrained specimen and contractant behavior for the loose samples.

4.2 Particle shape measurement results

By visual inspection and Powers (1953) roundness chart of the tailings samples the particle shape are subjectively classified to range from sub angular to very angular. The smaller fractions appear to be more angular compared to larger fraction.

Figure 4 presents the condensed results from the 2D image analysis. The analysis is done on samples split by five sieve sizes based on sieving, shape descriptors and its output values.

Table 4. The results from the basic geotechnical characterization and triaxial tests. Sample (-) is in this study only used for evaluation of strength properties

ID	a	-	b	C	d
Sample location	I	I	I	II	II
Sampling level [m]	13.3	20.0	13.3	8.3	16.8
Ocular classification	saSi	clSa	clSi	siSa	siCl
Initial state	Firm	Firm	Firm	Loose	Loose
Condition	Drained	Drained	Undrained	Drained	Drained
ρ [t/m ³]	1.96	1.97	1.93	1.76	1.89
w [%]	31-39	33-36	29-34	49-54	40-50
Initial conditions [kPa]					
$\sigma'_1 = \sigma'_3$	140	200	150	90	170
$\sigma_l = \sigma_3$	250	300	270	200	280
u	110	100	120	110	110
Compression rate. [mm/h]	1.0	0.9	2.0	0.6	0.6
Failure criterion	Max dev.str.	Max dev.str.	Max dev.str.	15% compr.	Max dev.str.
Compr. at failure [%]	10.4	9.6	14.2	15.0	14.4
σ'_1 at failure [kPa]	564	826	1170	484	794
σ'_3 at failure [kPa]	141	201	253	90	170
u at failure [kPa]	109	99	17	110	110
ϕ' (c = 0)	40°	37°	40°	43°	40°
ϕ' and c	c = 79 kPa, $\phi' = 29^\circ$			c = 39 kPa, $\phi' = 37^\circ$	

4.3 Particle shape measurement results

By visual inspection and Powers (1953) roundness chart of the tailings samples the particle shape are subjectively classified to range from sub angular to very angular. The smaller fractions appear to be more angular compared to larger fraction.

Figure 4 presents the condensed results from the 2D image analysis. The analysis is done on samples split by five sieve sizes based on sieving, shape descriptors and its output values.

AR and *Roundness* are inverse each other for individual measurement, if mean value is applied this relation is no longer valid. AR^{-1} was introduced and refers to the *AR* but in order to obtain an *AR* with range between 0 and 1 the conversion took place. Appendix contains a detailed table with the quantity values.

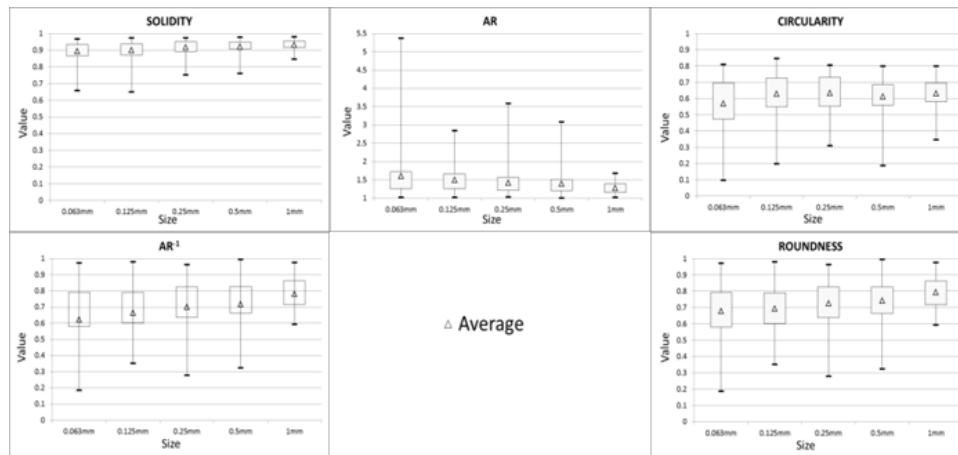


Figure 4: Box-plot for analyzed tailings material grouped by size determined by sieving

Median values were omitted in figures due to there is no significant difference to the average value (see appendix).

The complete database (the four tailing samples *a*, *b*, *c* and *d*) is presented in figure 4. It is visible in all quantities that bigger particles are more uniform. In general, for all quantities, the uniformity showed in big particles diminishes for smaller particles. It is also evident (in quantities ranging from 0 to 1) that the box plot (between 1st and 3th quartile), the average value and the *minimum* values move downwards in the vertical axis while the *maximum* values seem to have no apparent change (close to the upper limit).

Figure 5 compares the shape descriptor in the individual samples and figure 6 the individual samples variation by size for each shape descriptor. *AR* changes are more evident but it could be relative to the values range. In general *AR* decrease as the particle size increase. The rest of the quantities increase as the particles size increases. Sample *c* is possibly the exception due to this sample has no major changes when quantities are applied, in this sample oxidation was observed. *AR*⁻¹ and *Roundness* have exactly the same behavior, it is due to the fact both empirical relations represent the inverse of the *Aspect Ratio* (Ferreira and Rasband, 2012).

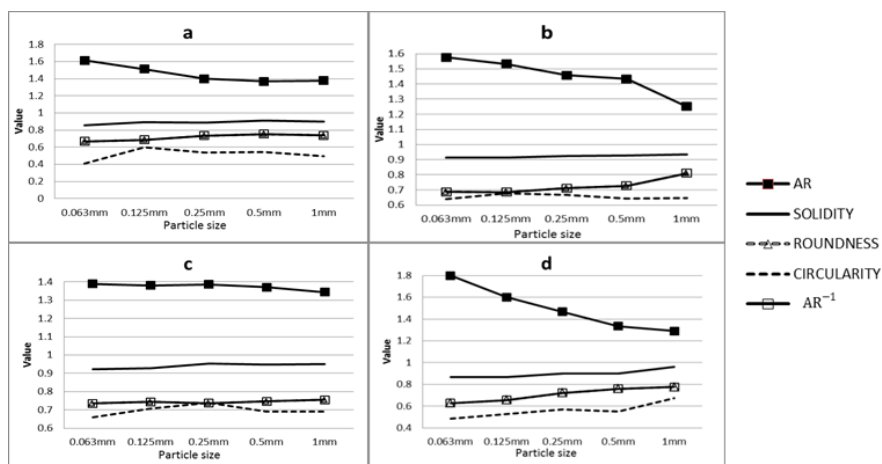


Figure 5. Mean value of descriptors for the different particle sizes in each tailings sample a-d. AR is the abbreviation for Aspect Ratio.

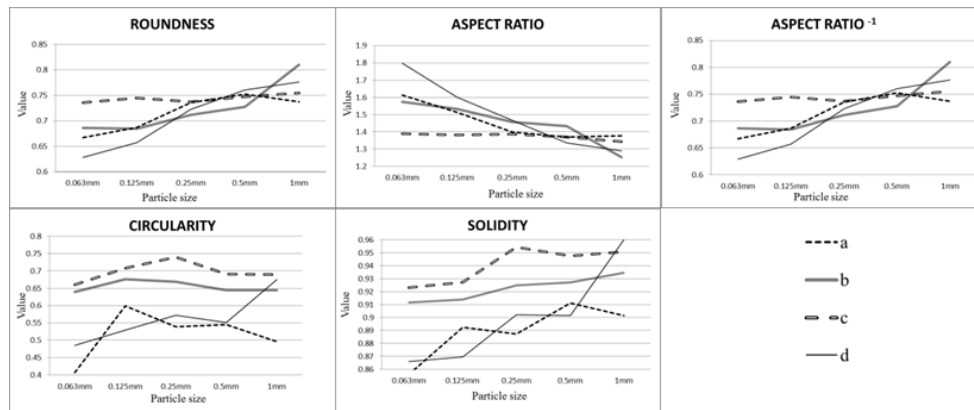


Figure 6. Mean value of the quantities in sample a-d and size based on sieving.

X-ray tests show that only sample *c* contains iron oxide in the form of Fe_xO_y . Solidity (fig. 6) is able to show the value increase when particle size increases in all samples while for the rest of the quantities it is not that defined for sample *c*. Sample *c* (oxidation presence as Fe_xO_y) does not show clear increase or decreases in values when quantities as *Roundness*, *Aspect Ratio* and *Aspect Ratio⁻¹* are applied. *Circularity* is showing a clear value increase on sample *d* while for the rest of the samples a higher peak value appears in some cases in small sizes and in others in medium sizes thus, from *Circularity* (except sample *d*) is not clear the size-shape increasing or decreasing behavior. *Roundness* and *AR⁻¹* have the same result and represents the inverses of the *AR* (see the mirror image comparing *AR* and *AR⁻¹*). Samples values on *Roundness* and *Aspect Ratio⁻¹* (except sample *c*) increase as particle size increase and for *Aspect Ratio* the values decrease as particle size increase (except sample *c*).

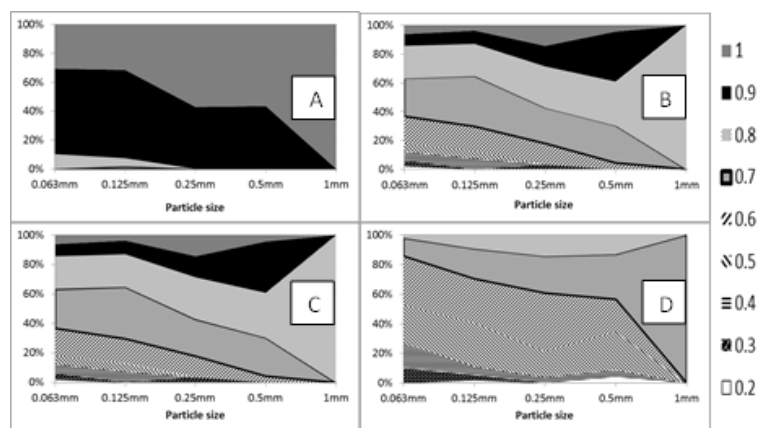


Figure 7. Percentages of the total particles by size and quantity value for sample *d* (A, *Solidity*; B, *Roundness*; C, *AR⁻¹* and D, *Circularity*)

Figure 7 present the relative amount of the analyzed particles (by size) that falls in the different ranges for A) *Solidity*, B) *Roundness*, C) *AR⁻¹* and D) *Circularity* for sample *d*. The results from samples *a* and *b* are similar as *d*, always appearing low values in the small fraction of size. Sample *c*, where oxidation is present contains more regular shape along the size fractions (see Fig. 5). It was decided to not show samples *a* and *b* in figure 7 due to the similarity with sample *d*. Also to sample *c* plotting was avoided because it presents no change on percentages along the sieving sizes resulting in a flat behavior.

4.4 Comparing friction angle and empirical relations

The results from the 2D-image analysis were applied in the equations 5 and 6 in table 3. Since all grains were analyzed the output was a range of numerical values of each shape descriptor. In this study was the average, minimum and maximum value of each shape descriptor tested in the equation. As reference to the output friction angle was the results from the triaxial tests on the samples in table 4. Table 5 and figure 8 shows that the *minimum* value of each shape descriptor presents less difference between the expected empirical friction angle ($\phi'_{\text{empirical}}$) and the laboratory tests output (ϕ'_{triaxial}). Among the quantities Circularity has the highest accuracy of predicted friction angle.

Table 5. The difference between the reference friction angle and the estimated friction angle

		$(\phi'_{\text{triaxial}} - \phi'_{\text{empirical}})$	
		$\phi'_{\text{triaxial}} - \phi'_{\text{empirical}} [^\circ]$	
Quantity		5	6
AR (converted to 0-1)	average	13.0	8.8
	maximum	14.5	11.1
	minimum	10.7	5.4
Circularity	average	12.3	7.8
	maximum	14.3	10.8
	minimum	8.6	2.3
Solidity	average	15.2	12.1
	maximum	15.8	13.1
	minimum	13.0	8.9
Roundness same as AR ⁻¹	average	13.3	9.3
	maximum	15.9	13.2
	minimum	10.9	5.7

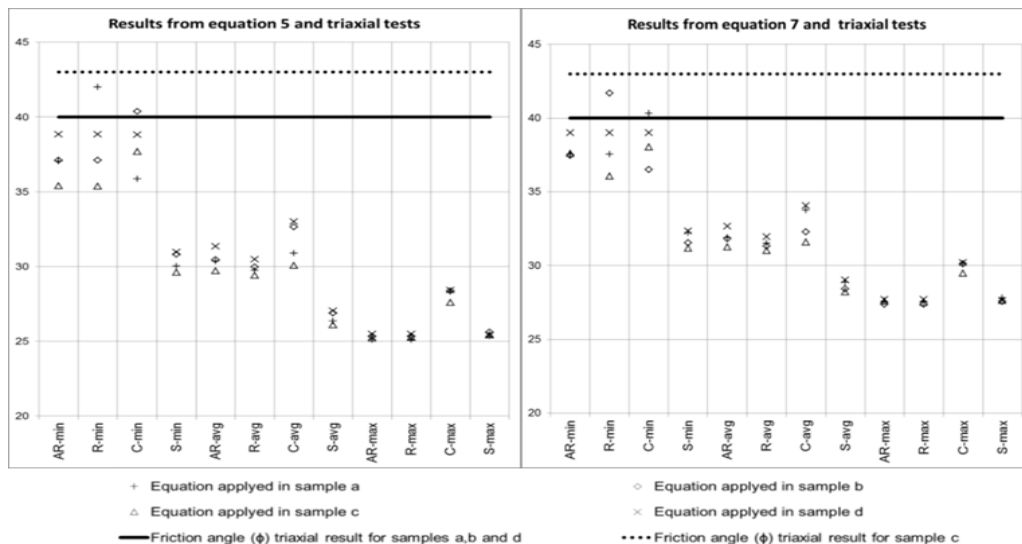


Figure 8. Friction angle results, lines represent the laboratory test (ϕ'_{triaxial}) and the points are the empirical relation output ($\phi'_{\text{empirical}}$).

5 Discussion

5.1 Particle shape measurement results

Tailings had been classified as very angular to sub angular material by visual inspection based on Powers (1953) comparison chart. The results of this classification collaborates with the conclusions of the general shape of tailings, e.g. by Garga et. al. (1984). The drawback with classification of shape by comparison chart is that the classification is subjective and difficult to quantify. There are other options to determine the angularity. Wadell (1932) is probably the most used and systematic method to determine the roundness, here the opposite to angularity, because it is focus in the corners configuration but still this methodology evolves in chart comparison. If any of the methodologies can be scripted and image analyzed roundness results would be more objective.

Small particles (<0.002mm) tend to be more platy and elongated (Mitchell and Soga, 2005) and this study shows how the elongated particles (relation 2:1, AR^{-1} value of 0.5) appear and populates the sample as much as 30% (fig. 7C) in the 0.063mm size, Circularity shows the increase of percentage to 50% with low circularity value of 0.5 for 0.063mm size (fig. 7D). The loom of elongated and irregular particles in sizes bigger than those declared by Mitchel and Soga (2005) could be due to that particles involve in this study are not natural geological materials but they are crushed and milled rock from the mining industry. The results of the ocular classification of the angularity also supports that the smaller particles are more irregular than the larger in this study.

Sample “c” was found to present some oxidation, presumable iron oxidation result of the acid leakage. The sample presents no change when quantities are used to determine the shape across the different sizes with exception of solidity. Solidity is probably detecting the surface changes (acid leakage dissolution) while the rest of the quantities do not, this relates the solidity with the third shape scale *surface texture*. Artificial breakage and fracture formation tend to follow the mineral surface along the weakest lines while acid leakage dissolves surface constituents. This could explain why Solidity is detecting changes in sample c while is not in the rest of the samples. The range that solidity involve (0.86-0.96 : 0.1 in difference) are quiet close, and the range suggest that the particles are quiet regular, this could be the result of the specific samples used and more samples should be included to determine the whole real workability range.

AR is the inverse of AR^{-1} and Roundness; the results show that the behavior between AR^{-1} and Roundness are exactly the same corroborating the Ferreira and Rasband (2013) description of these two quantities. As a result only one of these parameters is needed due to the inverse can be calculated easily. The inverse is applicable only for individual particles measurement and is not for e.g. the mean value (the mean value of a set of data among AR and Roundness will be not inverse each other). The use of these three quantities should depend on the nature of the work (if a range from zero to one is needed Roundness or AR^{-1} should be preferred). Roundness vs. AR choosing concerns more on the available data to calculate the quantity (Roundness and AR have the *major axis* in common and they also need the *area* and *minor axis* respectively, which data is available should be used) .

Circularity as Cox (1927) state relates the area and the perimeter of a particle with the area and perimeter that a circle should have (circle have area perimeter relation equal to one).

There are two inconvenient detected for circularity. 1) Length is the most influenced parameter by resolution (Schäfer, 2002) and perimeter is dependent on length, the error increases as the perimeter increases, it can be added that the quantity use the perimeter to the power of two increasing exponentially the error. Due to the fact that this parameter is influenced by the resolution it should be avoid when possible or use high resolution pictures. 2) Microscope focus for a 3 dimensional particle presents some challenges (characteristics used in the present research) due to the fact that on occasion is not possible to obtain a perfect defined outline of the particle having in this kind of pictures an irregular outline (instead of a regular straight defined line) that possible generates a longer perimeter as it should be.

5.2 Comparing friction angle empirical relations

In this study has previously published empirical relationships between shape and friction angle been evaluated in order to investigate if this methodology is possible to apply on tailings. Since the evaluated empirical relationships has been established on mainly uniformly graded sand and it is not likely that the actual resulting friction angle would be accurate predicted on tailings consisting of both smaller particles and a larger range in grain size distribution. The empirical relationships are based on the shape descriptor Roundness that can both been defined in different ways and also be evaluated differently. Cho et. al (2006) use the Roundness based on the Krumbein and Sloss (1963) modified chart and Rousé et. al (2008) uses the Roundness as Wadell (1932) defined based on a compilation of various authors. In this study has Roundness been automatically quantified by 2D-image analysis applying four different mathematical definitions; Circularity (C), Roundness (R), Solidity (S), and Aspect Ratio (AR). Despite the different methodologies applied to quantify or to qualitative classify the shape of the particles the trend of the friction angle should be similar if the shape descriptors are correct describing the material of interest.

Based on the general behavior of the empirical relations (eq. 5 and 6) the friction angle is likely to be higher in crushed artificial rock than for natural materials since crushed material in general are considered to be more angular (Garga et. al., 1984)

All quantities evaluated describe an underestimation of the reference friction angle from the triaxial tests. In all cases equations 5 and 6 presents maximum to minimum (in that order) difference in relation with the actual friction angle obtained in laboratory tests, been equation 6 the most suitable empirical relation to describe the friction angle for the samples. In the same way the value or statistical parameter *minimum* for the four quantities present the lowest differences. Underestimation is possible related with the empirical relations (table 3), the maximum value obtained from them is 42 degree and only one triaxial result was over this value (considering also the quantity value as zero). It can also explain that the *minimum* shape values produce the best agreement with the empirical relations. The limited amount of data shrinks the action area of the empirical relations but state an initial relation for further research and new data acquisition. All positive differences in table 5 represent the underestimation of the tailings friction angle that if apply in the design of tailings dams from the engineering perspective represent the safety of its stability.

As point out before the general trend of quantities is to increases in value (from zero to one) while the particle increase in size, it is applicable to individual samples (fig. 5) and for the overall data samples (fig. 4). In the same way empirical relations (eq. 5 and 7) friction angle (ϕ') increase while the quantities value decreases but, it is unknown if the gradient for both are related due to the lack of more triaxial test with lower friction angles. Data is only available for high friction angles and it is why the *minimum* values are relating better the empirical relation. Triaxial tests with material covering the range from very angular (quantity values close to zero) to rounded (quantity values close to 1) are required.

The best descriptor determined in this work depends on the final goal, e.g. the use of solidity should be limited to the third scale *surface texture* due to its ability to recognize differences in the surface. According to Schäfer (2002) lengths present relative error when measuring digital images the use of high resolution could diminish the error but the use of square parameters as in equation 1 and 2 could increase it.

Considering the assumed non-linearity in the Mohr-Coloumb failure envelope, especially for low effective stresses, the use of linear empirical relations between particle shape and friction angle will be valid only above, or in a specific range, of effective stress. The available data in this study is not sufficient to define any stress limits or suggest new empirical relations. But the demonstration of the methodology shows that it is possible to retrieve indicative material properties based on classification of the shape.

6 Conclusions

Based on the results in this study following conclusions can be draw:

It is possible by 2D-image analysis to automatically classify particle shape by different shape descriptors. By splitting a sample into different size ranges also multi size samples can be analyzed by this technique.

The investigated tailings are classified as sub angular to very angular. The smaller fractions, silt, appear to be more angular than larger fractions, here sand.

There are empirical relations between shape and friction angle that may be useful to predict friction angle based on the shape of tailings. The investigated previous published empirical relations between shape and friction angle in this study underestimates the reference friction angle obtained by triaxial tests.

7 Acknowledgements

This study was funded and supported by Boliden Ltd, Luleå University of Technology (LTU) and the University of Sonora (UNISON). The authors thank Lic. Eng. Kerstin Pousette at LTU for the triaxial testing of the tailings material.

8 References

- Al-Rawahy, Khalid. (2001). Tailings from mining activity, impact on groundwater, and remediation. *Science and Technology*. 6, 35-43.
- Bishop, A. W. and Wesley, L. D. (1975). A hydraulic triaxial apparatus for controlled stress path testing. *Géotechnique*. 25 (4), 657-670.
- Cheshomi, A., Faker, A. and Jones C.J.F.P. (2009). A correlation between friction angle and particle shape metric in quaternary coarse alluvia, *Quaternary journal of engineering geology and hydrogeology*. 42, 145-155.
- Cho G., Dodds, J. and Santamarina, J. C., (2006). Particle shape effects on packing density, stiffness and strength: Natural and crushed sands. *Journal of Geotechnical and Geoenvironmental Engineering*. 132 (5), 591-602.
- Cox, E. P. (1927). A method of assigning numerical and percentage values to the degree of roundness of sand grains. *Journal of Paleontology*. 1 (3), 179-183.
- Ferreira, Tiago and Rasband, Wayne (2012) ImageJ user guide.
- FHA (1997). User Guidelines for Waste and Byproduct Materials in Pavement Construction Publication Number FHWA-RD-97-148, U.S. Department of Transportation, Federal Highway Administration, Washington D.C.
- Folk, R. L. (1955). Student operator error in determining of roundness, sphericity and grain size. *Journal of Sedimentary Petrology*. 25, 297-301.
- Garga. Vinod. K.; ASCE, M. and McKay Larry. D. (1984) Cyclic Triaxial Strength of Mine Tailings. *Journal of Geotechnical Engineering*. 110 (8), 1091-1105.
- Holubec and D'Appolonia (1973). Effect of particle shape on the engineering properties of granular soils. *ASTM STP 523*, 304-318.
- Krumbein, W. C. and Sloss, L. L. (1963). *Stratigraphy and Sedimentation*, 2nd ed., W.H. Freeman, San Francisco.
- Mitchell, James K. and Soga, Kenichi (2005). *Fundamentals of soil behaviour*. Third edition. WILEY.
- Mora, C. F. and Kwan, A. K. H. (2000). Sphericity, shape factor, and convexity measurement of coarse aggregate for concrete using digital image processing. *Cement and Concrete Research*. 30 (3), 351-358.
- Powers, M. C. (1953). A new roundness scale for sedimentary particles. *Journal of Sedimentary Petrology*. 23 (2), 117-119.
- Rodriguez, J. M.; Edeskär T. and Knutsson S. (2013). Particle shape quantities and measurement techniques – A review. *Electronical Journal of Geotechnical Engineering*. 18 (A), 169-198.
- Rousé, P. C., Fennin, R. J. and Shuttle, D. A. (2008). Influence of roundness on the void ratio and strength of uniform sand. *Geotechnique*. 58 (3), 227-231.
- Shäfer, Michael (2002). Digital optics: Some remarks on the accuracy of particle image analysis. *Particle & Particle Systems Characterization*. 19 (3), 158-168.
- Sweco GEOLAB, 2007. Jordprovsanalys. Projekt Aitik labförsök. Uppdragsnummer 216-6092-310. Löp-nr 17095. In Swedish
- Wadell, H. (1932). Volume, Shape, and roundness of rock particles. *Journal of Geology*. 40, 443-451.

Yoginder, P. Vaid, Jing, C. Chern and Haidi, Tumi (1985). Confining pressure, grain angularity and liquefaction, Journal of Geotechnical Engineering. 111 (10), 1229-1235.

Appendix. Compilation of the min, max, mean and median shape quantities values in the four samples a-d.

sample	sieve size (mm)	number of samples	AR				Circularity				Roundness				Solidity			
			Min	Max	Mean	Median	Min	Max	Mean	Median	Min	Max	Mean	Median	Min	Max	Mean	Median
a	1	9	1.177	1.684	1.377	1.312	0.347	0.674	0.496	0.491	0.594	0.850	0.737	0.762	0.847	0.964	0.901	0.912
	0.5	28	1.020	2.093	1.369	1.306	0.263	0.722	0.546	0.564	0.478	0.981	0.752	0.766	0.760	0.965	0.911	0.922
	0.25	48	1.048	2.049	1.398	1.349	0.310	0.733	0.539	0.537	0.488	0.954	0.736	0.741	0.752	0.959	0.887	0.889
	0.125	93	1.077	2.316	1.513	1.427	0.239	0.802	0.599	0.598	0.432	0.929	0.687	0.701	0.780	0.962	0.893	0.899
	0.063	23	1.123	3.475	1.613	1.458	0.097	0.636	0.407	0.410	0.288	0.890	0.667	0.686	0.658	0.933	0.856	0.879
b	1	55	1.025	1.683	1.251	1.230	0.451	0.799	0.645	0.646	0.594	0.975	0.810	0.813	0.859	0.981	0.935	0.936
	0.5	52	1.006	3.086	1.433	1.361	0.469	0.762	0.644	0.642	0.324	0.994	0.727	0.735	0.861	0.967	0.927	0.927
	0.25	53	1.038	2.113	1.457	1.375	0.491	0.803	0.668	0.681	0.473	0.964	0.712	0.727	0.823	0.968	0.925	0.929
	0.125	66	1.033	2.843	1.532	1.423	0.413	0.797	0.676	0.684	0.352	0.968	0.684	0.703	0.741	0.959	0.914	0.926
	0.063	67	1.036	3.413	1.575	1.377	0.361	0.805	0.639	0.667	0.293	0.965	0.686	0.726	0.705	0.969	0.912	0.931
c	1	8	1.069	1.569	1.344	1.357	0.579	0.757	0.690	0.711	0.637	0.936	0.755	0.738	0.906	0.975	0.951	0.959
	0.5	22	1.015	2.051	1.370	1.341	0.620	0.786	0.691	0.681	0.488	0.985	0.747	0.746	0.890	0.963	0.948	0.951
	0.25	43	1.049	1.858	1.386	1.361	0.622	0.805	0.739	0.747	0.538	0.953	0.737	0.735	0.891	0.975	0.954	0.959
	0.125	65	1.021	2.561	1.381	1.346	0.273	0.848	0.707	0.751	0.390	0.980	0.744	0.743	0.729	0.974	0.927	0.948
	0.063	39	1.045	2.151	1.373	1.302	0.334	0.810	0.654	0.687	0.465	0.957	0.743	0.768	0.779	0.967	0.919	0.925
d	1	3	1.257	1.350	1.290	1.263	0.659	0.687	0.675	0.680	0.741	0.796	0.776	0.792	0.948	0.967	0.960	0.965
	0.5	23	1.058	1.712	1.336	1.314	0.188	0.800	0.552	0.550	0.584	0.945	0.760	0.761	0.821	0.978	0.901	0.913
	0.25	28	1.047	3.585	1.467	1.400	0.343	0.770	0.573	0.564	0.279	0.955	0.723	0.715	0.835	0.958	0.902	0.907
	0.125	54	1.031	2.817	1.601	1.514	0.199	0.765	0.530	0.534	0.355	0.970	0.657	0.661	0.650	0.944	0.870	0.879
	0.063	49	1.028	5.369	1.799	1.580	0.230	0.704	0.485	0.491	0.186	0.972	0.629	0.633	0.742	0.950	0.866	0.875